

ROLE OF THE COST FUNCTION FOR MATERIAL PARAMETER ESTIMATION

Patrick Lauer¹, Tristan Hehnen^{2,3}, Corinna Trettin², Fabian Brännström¹ and Lukas Arnold^{2,3}

¹ Fire Technology and Fire Safety Engineering, University of Wuppertal, Germany

² Computational Civil Engineering, Bergische Universität Wuppertal, Germany

³ Institute for Advanced Simulation, Forschungszentrum Jülich, Germany

ABSTRACT

Cost functions in optimisation processes are used as a measure to compute the distance between two data sets. Commonly, the root mean square error is used as a cost function for the estimation of material parameters based on bench-scale experiments. Due to the noise and variance in the target experimental data, this may not be the best choice. This contribution presents three other approaches, which are implemented into the PROPTI framework. Their application is demonstrated on experiments with a PMMA sample in a controlled atmosphere pyrolysis apparatus (CAPA II). Although, in the specific case investigated here, the impact of the various cost function classes is small, a benefit is expected for other samples with varying complexity.

INTRODUCTION

Inverse modelling of bench-scale experiments is a common method to determine material parameters for pyrolysis simulation [1], e.g. to compute flame spread. An important part in the inverse modelling process (IMP) is the cost function. It determines the deviation between target data and a model response, e.g. between experimental data and simulation results.

In this contribution, several different cost functions are evaluated for determining material parameter sets that allow the simulation of pyrolysis of solid polymers. Basis for this assessment is the inverse modelling tool PROPTI [2, 3]. Its functionality has been expanded by implementing additional cost functions, apart from the earlier default root mean square error (RMSE). Furthermore, multiple cost functions can now be combined and weighted individually, to allow putting emphasis on specific features in the data. It is also possible, to take different experiments into account at once and influence their respective contributions by assigning weights.

The added cost functions are:

- normalised root square error (NRSE) for individual points,
- threshold for single points (THR),
- RMSE applied to a range, e.g. percentage, enveloping the target data (RANGE), and
- RMSE applied to a band enveloping the target data, e.g. minimum and maximum values per time step of multiple repetitions of an experiment (BANDS).

The numerical modelling was conducted with the Fire Dynamics Simulator FDS [4], version 6.7.4 is used. A data set [5] is provided in addition to this article. It contains the input files for the the IMP runs and FDS simulations, their respective results as well as further Python scripts used for the analysis of the data.

MATERIALS AND METHODS

Inverse Modelling Process

The IMP is conducted with the open-source inverse modelling framework PROPTI [6]. This framework handles the communication between an optimisation algorithm and a simulation model on a computing cluster, e.g. here the supercomputer JURECA [7]. As optimisation algorithm the shuffled complex evolutionary algorithm developed by Duan et al. [8] is chosen, as implemented in SPOTPY [9]. A more detailed description of how this process is generally set up can be found in [2, 3].

Micro- and bench-scale fire tests of consumer-grade black poly methyl methacrylate (PMMA), performed by various international laboratories from the "Condensed Phase Material Database" [10] was chosen as IMP targets. Specifically, thermogravimetric analysis (TGA) data from the University of Lille - ENSCL - Unite Materiaux et Transformations (UMET) and Controlled Atmosphere Pyrolysis Apparatus II (CAPA II) [11] data from the University of Maryland (UMD) are applied for this evaluation.

The IMP is conducted with a simplified simulation setup of the CAPA II. Focus is set on determining the thermophysical parameters, i.e. density, emissivity, conductivity and specific heat capacity. Reaction kinetics, utilising an Arrhenius model as implemented in FDS, are treated as known parameters. These have been estimated in a initial step, via an individual IMP, and are not adjusted any further when focusing on the CAPA II case. For this first step, the built-in TGA model of FDS (`TGA_ANALYSIS=.TRUE.`) is used to run the individual simulations. TGA data from UMET [10] is used as target. Specifically, three experiments are chosen, with heating rates of 1 K/min, 10 K/min and 50 K/min. During the IMP, each generated parameter set is subjected to a simulation of each of the experimental conditions mentioned above. Its combined performance for all three conditions is then used as fitness value for the cost function. Following this process, reaction kinetics parameters for each of the two identified decomposition reactions are determined.

The simplified simulation setup of the CAPA II is based on the simplified Cone Calorimeter setup that was used in [3]. The focus is solely set on the mass loss of the PMMA sample, thus the gas phase is ignored to cut down on the computational demand, i.e. `SOLID_PHASE_ONLY=.TRUE..` To control artefacts in the mass loss data, the solid phase cells are adjusted for the PMMA surface layer. The `CELL_SIZE_FACTOR` is set to 0.05, reducing the cell size by a factor of 20 of the automatically computed FDS default. The `STRETCH_FACTOR` is set to 1, to ensure a uniform cell size across the layer thickness.

To replicate the two reaction steps of PMMA in FDS, two materials are defined (`MATL`) that each produce a solid residue and methane as combustible gaseous species. Each of the materials gets assigned a set of the reaction kinetics parameters based on the previous TGA-IMP. The solid residue is assumed to be around 0.1 % of the original sample mass. From the total sample mass about 2.5 % contribute to reaction A, while the remaining 97.5 % contribute to reaction B. Both materials are mixed in a surface (`SURF`) layer according to their respective contributions, representing the PMMA slab. A thin layer is added to the back side, representing a copper foil, as per description of the experiment and apparatus [10, 11].

The thermophysical parameters are determined in three groups of IMP runs that only differ in the utilised cost function: `BANDS`, `RANGE` and `RMSE`. The test condition in the CAPA II is replicated by assigning an `EXTERNAL_FLUX` of 25 kW/m² to the sample surface.

The cost function `BANDS` defines a band around the target data. Adding and subtracting a desired value from the target data created the lower and upper limit of the band. These limits have been pre-computed and are provided to PROPTI as two data series in an external text file. The limits are defined by the variance data provided with the data from the experiments. With `RANGE` a lower and upper limit of 5.0 % are computed by PROPTI itself. These methods assume a perfect fit for data points of the model

that are located within the area defined by the limits. With increasing distance to the target area the penalty increases as well. For RMSE the divergence between the two data series of the model and the experiment is computed directly. Here, a perfect fit is only achieved when the data points of the model and the experiment match exactly. More detailed explanations on the cost functions are provided in the following section. For each of the four cost functions 25 repetitions of the IMP run are conducted. This allows to estimate the variability induced by the non-deterministic character of the optimisation algorithm.

Furthermore, a validation step is conducted with experimental data that was not used for the optimisation process. The best parameter sets of each IMP run are utilised in a simulation setup with an external flux of 60 kW/m².

Evaluation Methods

The IMP aims to minimise the differences between experimental observations and model predictions to estimate the input parameters so the model generates an output with the least possible difference to the experimental observations. Thus, a mathematical formulation that quantifies the difference between the data of the experiment and the model as a cost function is needed, which is then minimised during the IMP. A combined cost function can be established based on individual cost functions, which act on a single data set or multiple data sets.

Single point

One single point can be defined as objective. The error is the distance between the experimental value y and the modelled value \hat{y} normalised to y as shown in equation 1 and visualised in figure 1a.

$$\text{NRSE} = \frac{|\hat{y}_t - y_t|}{y_t} \quad (1)$$

For example, this could be used for temperature at ignition time. By increasing the number of optimised parameters, the width of the solution will increase. Several parameter sets may fit to the objective single point and local optima are sufficient for a perfect fit.

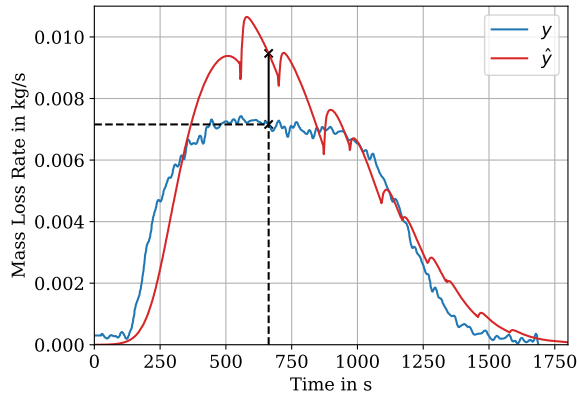
Threshold

The threshold method is very similar to the single point approach. The first time $\hat{y}(t)$ exceeds (equation 2) or goes below (equation 3) $y(t_0)$, is used to calculate the normalised distance on t-axis between these two values. If the condition is never met, the assumption is that always the largest difference is applied. A visual example is provided in figure 1b.

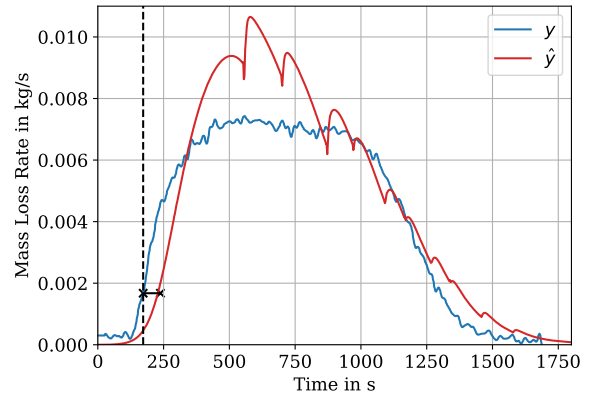
$$\text{THR}_{min} = \min \left\{ |\{t|\hat{y}(t) > y(t_0)\} - t_0|, \max\{|t_{min} - t_0|, |t_{max} - t_0|\} \right\} / t_0 \quad (2)$$

$$\text{THR}_{max} = \min \left\{ |\{t|\hat{y}(t) < y(t_0)\} - t_0|, \max\{|t_{min} - t_0|, |t_{max} - t_0|\} \right\} / t_0 \quad (3)$$

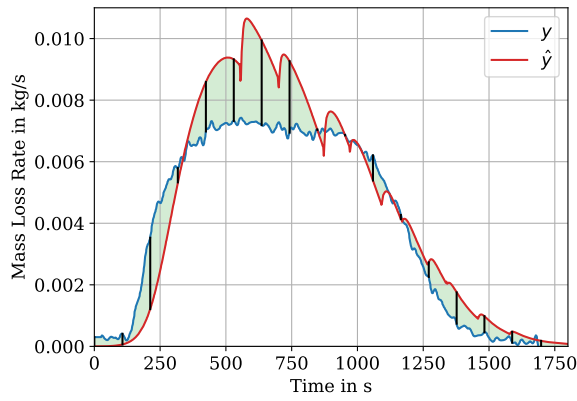
Such a cost function based on equation 2 could be the time of ignition, for example. The mass loss rate or heat release rate will increase by a certain threshold after a defined point in time (t_0), while its further temporal development is ignored, i.e. not represented in the cost function, by the IMP.



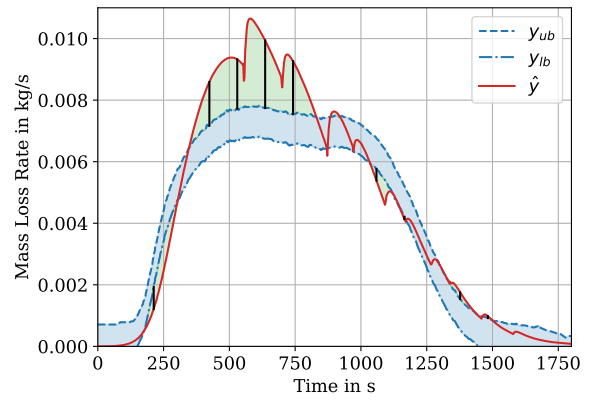
(a) Single Point NRSE



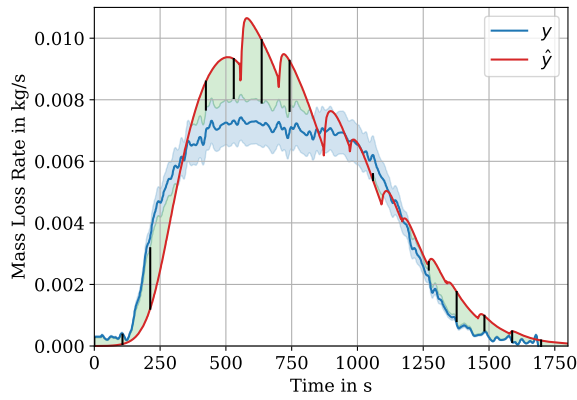
(b) Single Point Threshold



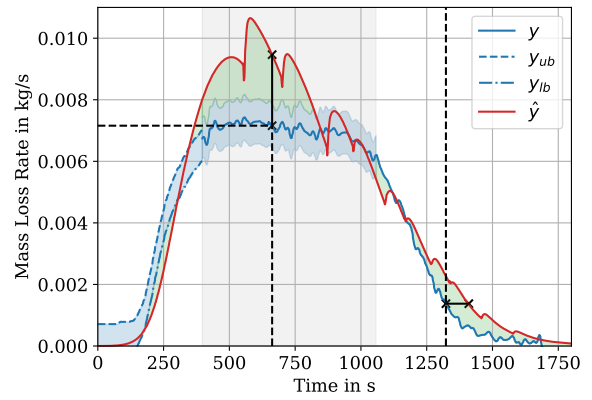
(c) RMSE



(d) RMSE BANDS



(e) RMSE RANGE



(f) Combined

Figure 1: Examples of evaluation functions. Target data marked in blue and model response marked in red. Areas marked in green indicate the distance between model response and target. Blue areas indicate the target area.

Table 1: Options for normalisation parameter y_N

RMSE	NRMSE	CV(RMSE)	IQRMSE
$y_N = 1$	$y_N = y_{max} - y_{min}$	$y_N = \bar{y}$	$y_N = CDF_y^{-1}(0.75) - CDF_y^{-1}(0.25)$

Table 2: Options for comparison value Δy_t

RMSE	$\Delta y_t = \hat{y}_t - y_t$
BANDS	$\Delta y_t = \begin{cases} 0 & \text{for } y_{t,lb} \leq \hat{y}_t \leq y_{t,ub} \\ \hat{y}_t - y_{t,lb} & \text{for } \hat{y}_t < y_{t,lb} \\ \hat{y}_t - y_{t,ub} & \text{for } \hat{y}_t > y_{t,ub} \end{cases}$
RANGE	$\Delta y_t = \begin{cases} 0 & \text{for } (1-r)y_t \leq \hat{y}_t \leq (1+r)y_t \\ \hat{y}_t - (1-r)y_t & \text{for } \hat{y}_t < (1-r)y_t \\ \hat{y}_t - (1+r)y_t & \text{for } \hat{y}_t > (1+r)y_t \end{cases}$

Root mean square error

Root mean square error (RMSE) as shown in equation 4 is a measure for the difference between values of two data sets, which contain n_y data points. Figure 1c shows an exemplary mass loss rate of an irradiated sample as a function of time with experimental values y and model values \hat{y} . Since the raw RMSE ($y_N = 1$) is scale dependent and cannot be compared to other values, RMSE needs to be normalised. Table 1 provides different values for the normalisation variable y_N , where y_N can be the mean (coefficient of variation of the RMSE, CV(RMSE)), the range (normalised RMSE, NRMSE) or the difference between the first and third quartile (interquartile RMSE, IQRMSE) of y .

Another aspect of the cost function is the induced stiffness. A strict comparison of experimental and simulation data will never reach zero values, i.e. perfect fitting. To face this aspect, a cost function that uses a data band is introduced. Assuming uncertainties in the experimental and simulation data, this is not limiting the quality of the inverse modelling. Yet, a less stiff system could lead to benefits like quicker convergence and robust solutions. Table 2 introduces two different concepts to cover this. BANDS rates any value between a lower and upper boundary as perfect fit ($\Delta y_t = 0$) for a given point, otherwise it uses the actual distance. An example of this is shown in figure 1d with lower and upper experimental values as y_{lb} and y_{ub} . RANGE rates \hat{y} with a deviation of r to y as perfect fit, otherwise it uses the actual distance. Figure 1e shows an example.

$$RMSE = \frac{1}{y_N \sqrt{n_y}} \sqrt{\sum_{t=1}^{n_y} (\Delta y_t)^2} \quad (4)$$

Cost function formulation

The composition of the total error E , the total cost function, is formulated in equation 5 as the sum of each single element weighted by an individual weighting factors w for each partial cost function in the according groups (I, J, K). Figure 1f shows an example of this combination in a single data set, albeit this approach is not fixed to a single data set, but can cover multiple experimental and model setups.

Table 3: Reaction kinetics parameter set for a two-step decomposition determined from TGA data of UMET [10].

Arrhenius Parameter	Value	Unit
Reaction A		
<i>A</i>	9.98e+04	1/s
<i>E</i>	6.24e+04	kJ/kmol
Reaction B		
<i>A</i>	1.00e+11	1/s
<i>E</i>	1.60e+05	kJ/kmol

$$E = \sum_{i=0}^I (w_i \cdot \text{RMSE}_i) + \sum_{j=0}^J (w_j \cdot \text{THR}_j) + \sum_{k=0}^K (w_k \cdot \text{NRSE}_k) \quad (5)$$

EVALUATION

Reaction Kinetics Data

The reaction kinetics parameters, based on UMET TGA experiments [10], are presented in table 3. The reaction order n is set to 1. For a qualitative comparison, the normalised residual masses and mass loss rates are provided in figure 2. Solid lines mark the data from the experiment and dashed lines mark the simulation response. These parameters are applied unchanged in all further IMP runs that are used to determine the thermophysical material parameters.

Thermophysical Properties

The resulting thermophysical parameters for the different cost functions are provided in table 4. This table shows the mean values for each parameter across 25 repetitions of the IMP and the respective variance. Furthermore, the best parameter set within each group is listed. It should be noted, that the estimated parameters are not necessarily physical but effective parameters. The respective sampling limits utilised during all IMP runs are provided in table 6 in the appendix.

Figure 3 shows a comparison between the mass loss rate of the CAPA II experiment at 25 kW/m² and the simulation response of the IMP groups. All responses are very close to each other, thus only the best parameter set from each group is shown.

The results of the validation simulation at 60 kW/m² are shown in figure 4. Only the responses of the best parameter sets of each group are plotted, as well as the CAPA II data from the 60 kW/m² experiment [10]. In general, the responses are very similar to each other as in the 25 kW/m² case. However, all cases show significant fluctuations before the material is used up. For the cost functions RANGE and RMSE minor fluctuations can also be observed over nearly the full duration of the simulation.

DISCUSSION

In this contribution, different cost functions are investigated with respect to their performance in finding material parameter sets. For the chosen example case here, none of the different cost functions significantly outperforms any of the others. The best parameter sets within each cost function group, as well as

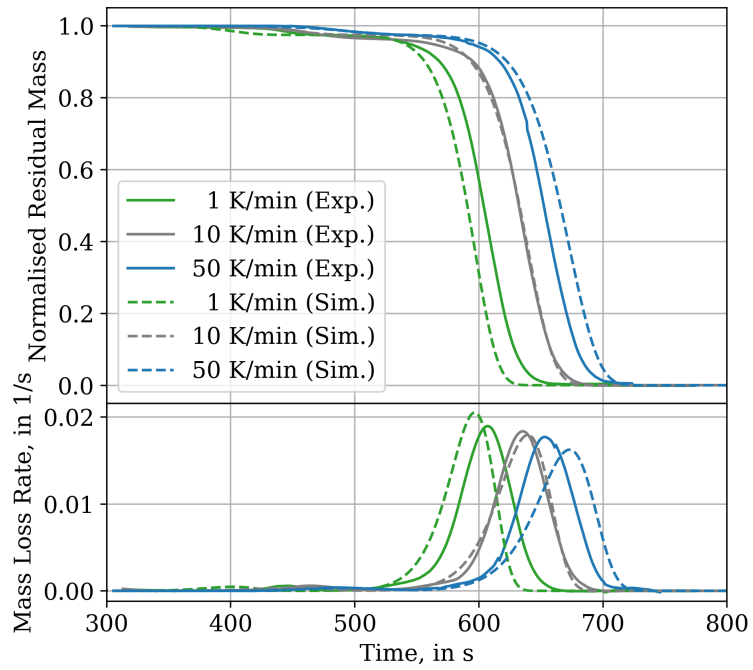


Figure 2: Comparison between TGA experiments by UMET [10] (Exp.) and the best parameter set of the IMP run that determined the reaction kinetics parameters (Sim.).

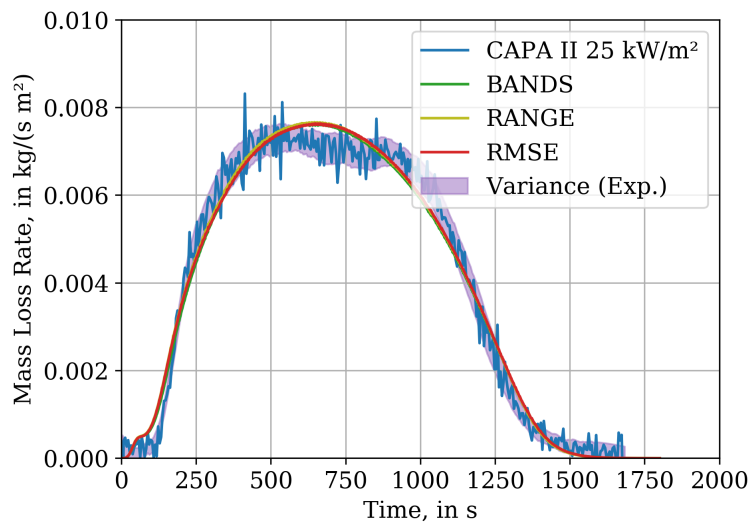


Figure 3: Comparison between CAPA II experiment [10] and the best parameter sets of the IMP runs with different cost functions.

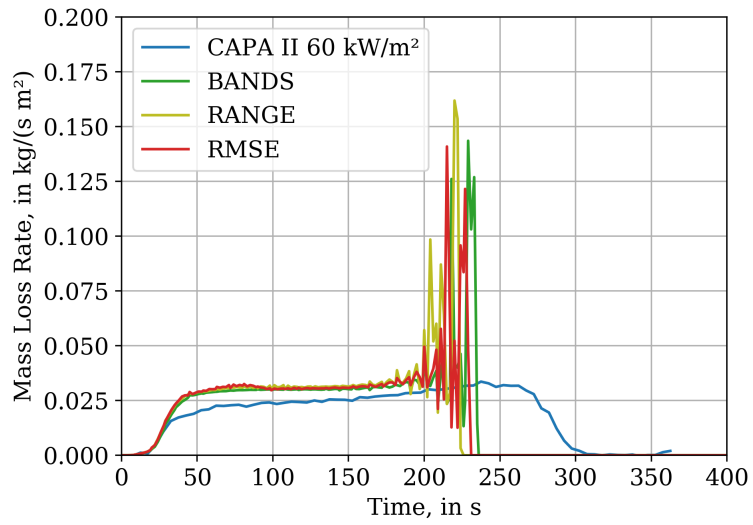


Figure 4: Comparison between CAPA II experiment [10] and the best parameter sets of the IMP runs with different cost functions as validation cases.

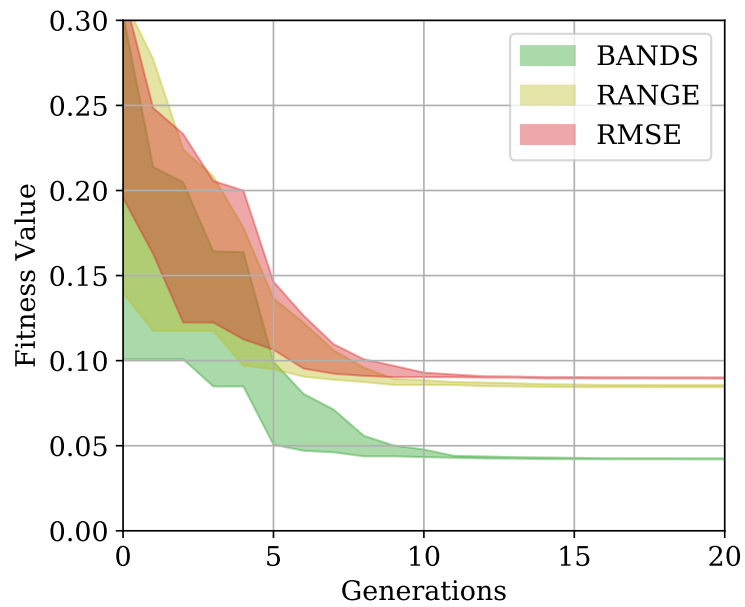


Figure 5: Cumulative minimum areas for the three cost functions over 25 repeated IMP runs for each cost function. Note: The individual plots are not directly comparable due to their different cost functions.

Table 4: Thermophysical properties, 25 repetition for each of the three cases (RMSE, RANGE, BANDS). Symbols and units are described in the appendix, table 5.

Param.	RMSE			RANGE			BANDS		
	best	mean	σ	best	mean	σ	best	mean	σ
fit	0.0892	0.0897	0.0002	0.0838	0.0846	0.0004	0.0417	0.0421	0.0002
ρ_a	1201.3	1204.5	1.3	1200.5	1205.0	3.1	1194.8	1196.0	0.8
k_a	0.1083	0.1133	0.0021	0.1075	0.1125	0.0037	0.1160	0.1213	0.0030
$c_{p,a}$	2.6037	2.7065	0.0241	2.5920	2.6909	0.0268	2.6575	2.6986	0.0167
ϵ_a	0.9298	0.9694	0.0109	0.9322	0.9656	0.0139	0.9451	0.9691	0.0110
Δh	669.2	704.3	12.3	676.6	703.0	14.7	675.2	709.1	16.3
ρ_r	716.4	1162.1	159.2	897.1	1161.5	132.1	797.3	1117.5	163.0
k_r	0.2162	0.3349	0.0690	0.2053	0.3334	0.0623	0.1871	0.3268	0.0691
$c_{p,r}$	0.7873	1.1876	0.2455	0.7970	1.2755	0.2488	0.8056	1.2873	0.3065
ϵ_r	0.9871	0.9890	0.0009	0.9837	0.9877	0.0018	0.9867	0.9888	0.0009

across these groups, show nearly the same simulation response. The variances between 0.0002 to 0.0004 for the fitness values in the different groups indicate that the different methods yield robust results. Looking at the cumulative minimum of the fitness values, none of the discussed cost functions stands out in terms of how fast they converge to their respective minimum. All need about 11 generations to converge, see figure 5. Thus, no useful statement as to how fast convergence is reached can be made here.

For a larger number of optimisation parameters this behaviour might be different, as compared to the nine optimisation parameters used here. Also, larger sampling limits for the individual parameters might have a stronger effect on the convergence when choosing different cost functions. Furthermore, the experiments were conducted in an inert atmosphere and in the simulations the gas phase reactions were neglected. This could contribute to an oversimplified modelling of the involved processes, leading to a more trivial case. Nevertheless, a cost function that uses an area as a target, provides means to incorporate the uncertainty observed in the experiments. It should be pointed out, however, that it seems to be beneficial to apply some smoothing to target area limits. Thus, the algorithm is not influenced by the local fluctuations and more focused towards finding a global structure. This is indicated by the area in figure 3, when directly compared to the noisy results of the experiment.

The default method of comparing two data series directly per RMSE is considered a more rigid cost function than BANDS and RANGE. Primarily, because RMSE requires exact matches of the data points, while slight variations in the other cases could still fall inside the target area. BANDS and RANGE could be useful to account for variance that is encountered when repeating a single experiment multiple times and allow for its representation during the IMP.

The ability to combine cost functions in different ways, allows to target multiple values, like heat release rate or surface temperature, and their unique features, like heat release peaks on different experimental setups (e.g. different heat fluxes or gas atmospheres), as these may be of crucial importance for the real-scale applications, especially for flame spread modelling.

DATA SET

This contribution is accompanied by a data repository [5], hosted via Zenodo. It contains the complete data of each IMP run, simulations of the best parameter sets of each IMP run, the IMP run for the reaction

kinetics parameters, the validation simulations, the plots shown in the article and presentation, as well as the Jupyter Notebooks used for the data analysis.

Note: The copper foil thickness is set to 0.2 mm in all simulations, due to a typo in the FDS input file template and should have been 0.025 mm according to [11]. A simulation with the correct thickness showed very little divergence from the conducted simulations, thus the effect of the typo is regarded to be neglectable. Therefore, all files in the accompanying data repository are using the incorrect initial value. The mentioned simulations and a plot comparing both results are provided in the repository.

ACKNOWLEDGEMENTS

The authors gratefully acknowledge the computing time granted (project: cjjsc27; application number: 19595) by the JARA-HPC Vergabegremium and VSR commission on the supercomputer JURECA at Forschungszentrum Jülich [7, 12].

References

- [1] Mohammed M. Khan, Archibald Tewarson, and Marcos Chaos. Combustion characteristics of materials and generation of fire products. In Morgan J. et al. Hurley, editor, *SFPE Handbook of Fire Protection Engineering*, pages 1143–1232. Springer New York, New York, NY, 2016. doi: 10.1007/978-1-4939-2565-0_36. URL http://dx.doi.org/10.1007/978-1-4939-2565-0_36.
- [2] Lukas Arnold, Tristan Hehnen, Patrick Lauer, Corinna Trettin, and Ashish Vinayak. Propti—a generalised inverse modelling framework. In *Journal of Physics: Conference Series*, volume 1107, page 032016. IOP Publishing, 2018.
- [3] Lukas Arnold, Tristan Hehnen, Patrick Lauer, Corinna Trettin, and Ashish Vinayak. Application cases of inverse modelling with the propti framework. *Fire Safety Journal*, page 102835, 2019. ISSN 0379-7112. doi: <https://doi.org/10.1016/j.firesaf.2019.102835>. URL www.sciencedirect.com/science/article/pii/S0379711219300438.
- [4] Kevin McGrattan, Simo Hostikka, Jason Floyd, Randall McDermott, and Marcos Vanella. *Fire Dynamics Simulator User’s Guide, version 6.7.4*, 3 2020.
- [5] Patrick Lauer, Tristan Hehnen, Corinna Trettin, Fabian Brännström, and Lukas Arnold. Role of the Cost Function for Material Parameter Determination - Data Set, 8 2020. URL <https://zenodo.org/record/3987799>.
- [6] Lukas Arnold, Tristan Hehnen, Patrick Lauer, Corinna Trettin, and Ashish Vinayak. Propti, 3 2018. URL <https://zenodo.org/record/1438349>.
- [7] Jülich Supercomputing Centre. Jureca: General-purpose supercomputer at jülich supercomputing centre. *Journal of large-scale research facilities*, 2, 2016. URL <http://dx.doi.org/10.17815/jlsrf-2-121>.
- [8] Q Y Duan, Vijai K Gupta, and Soroosh Sorooshian. Shuffled complex evolution approach for effective and efficient global minimization. *Journal of optimization theory and applications*, 76(3): 501–521, 1993.
- [9] Tobias Houska, Philipp Kraft, Alejandro Chamorro-Chavez, and Lutz Breuer. Spotting model parameters using a ready-made python package. *PloS one*, 10(12):e0145180, 2015.

- [10] Randall McDermott and Isaac Leveton (Editors). Measurement and Computation of Fire Phenomena (MaCFP): Condensed Phase Material Database, 11 2019. URL <https://github.com/MaCFP/mat1-db>. Commit: 7335c4470ec2cb0327ac0fe8386ecfeee6b3c6b1.
- [11] Joshua D. Swann, Yan Ding, Mark B. McKinnon, and Stanislav I. Stoliarov. Controlled atmosphere pyrolysis apparatus ii (capa ii): A new tool for analysis of pyrolysis of charring and intumescent polymers. *Fire Safety Journal*, 91:130 – 139, 2017. ISSN 0379-7112. doi: <https://doi.org/10.1016/j.firesaf.2017.03.038>. URL <http://www.sciencedirect.com/science/article/pii/S0379711217300541>. Fire Safety Science: Proceedings of the 12th International Symposium.
- [12] Dorian Krause and Philipp Thörnig. JURECA: Modular supercomputer at Jülich Supercomputing Centre. *Journal of large-scale research facilities*, 4:A132, 2018. doi: 10.17815/jlsrf-4-121-1.

1 APPENDIX

1.1 Symbols Overview

Table 5: Symbols Overview

Name	Symbol	Unit
Activation Energy	E	kJ/kg
Density	ρ	kg/m ³
Emissivity	ϵ	-
Heat Of Reaction	Δh	kJ/kg
Mass Loss Rate	MLR	kg/(s · m ²)
Pre-exponential Factor	A	1/s
Temperature	T	°C
Thermal Conductivity	k	m/K
Time	t	s
Specific Heat Capacity	c_p	kJ/(kg · K)
Standard Deviation	σ	same as the data
Reaction Order	n	-

1.2 Sampling Limits

Table 6: Sampling limits used for the IMP runs RMSE, RANGE and BANDS.

Parameter	Lower Limit	Upper Limit
ρ_a	600.000	1500.000
k_a	0.090	0.350
$c_{p,a}$	0.875	2.725
ϵ_a	0.010	0.990
Δh	250.000	1550.000
ρ_r	500.000	1500.000
k_r	0.090	0.550
$c_{p,r}$	0.500	2.000
ϵ_r	0.010	0.990